AIP | Journal of Applied Physics

Free electron terahertz wave radiation source with two-section periodical waveguide structures

Weihao Liu, Sen Gong, Yaxin Zhang, Jun Zhou, Ping Zhang et al.

Citation: J. Appl. Phys. **111**, 063107 (2012); doi: 10.1063/1.3696969

View online: http://dx.doi.org/10.1063/1.3696969

View Table of Contents: http://jap.aip.org/resource/1/JAPIAU/v111/i6

Published by the American Institute of Physics.

JOURNAL OF APPLIED PHYSICS **111**, 063107 (2012)

Free electron terahertz wave radiation source with two-section periodical waveguide structures

Weihao Liu,[a)] Sen Gong, Yaxin Zhang, Jun Zhou, Ping Zhang, and Shenggang Liu
Terahertz Science and Technology Research Center, University of Electronic Science and Technology of China, Chengdu 610054, China

(Received 20 December 2011; accepted 24 February 2012; published online 26 March 2012)

We analyze a free electron terahertz wave radiation source with two-section periodical waveguide structure (PWS), where the first section (section-I) is used to pre-modulate the electron beam and the second section (section-II) is for terahertz wave generation. By means of theoretical analysis and numerical simulations, we demonstrate that the starting current density of the beam-wave interaction in section-II can be significantly reduced provided that the operation frequency is the harmonic of electron beam's pre-modulation frequency. This kind of source can generate relatively high power terahertz wave radiation but only need moderate beam current density. And it may have great potential application in developing the compact and high power terahertz wave radiation source. © *2012 American Institute of Physics*. [http://dx.doi.org/10.1063/1.3696969]

I. INTRODUCTION

Terahertz wave, electromagnetic radiation in the frequency from 0.1 THz to 10 THz (wavelength of 3 mm down to 0.03 mm), has attracted extensive interests of scientists from different disciplines for its great potential applications in varieties of fields of modern science. Yet till now, it is still an urgent problem to develop the compact, room temperature, and relatively high power terahertz radiation source, even though great efforts have been made.[1–10]

Traditional vacuum electronic devices, such as backward wave oscillator (BWO) and extended interaction oscillator (EIO),[11,12] can generate radiation with milliwatt to watt power level in the low frequency terahertz regime, and they are also the most commonly used radiation sources in real applications. But it is hard for this kind of devices to reach the high frequency terahertz region (higher than 0.5 THz) due to the requirement of extremely high starting beam current density.[11]

The diffraction radiation from the periodical waveguide structure (PWS) excited by a uniformly moving electron beam was experimentally presented in Ref. 13 in 2009. And its mechanism was found in Ref. 14, which demonstrated that it is due to the coupling of electron beam with the waveguide modes in the PWS. Without the requirement of starting current density, this kind of radiation may offer a good opportunity to the vacuum electronics and bring attractive prospects to develop the compact and tunable free-electron-radiation-source in the high frequency terahertz regime. The terahertz radiation source based on this mechanism was explored in Ref. 15, in which the pre-modulated electron beam (train of electron bunches) was proposed to improve the radiation power and efficiency. It showed that the radiation power and efficiency will be significantly enhanced provided that the coherent radiation from the pre-modulated electron beam is achieved.

In this paper we propose the concept of two-section PWS to pre-modulate the electron beam and generate coherent terahertz wave radiation. The scheme and its theoretical analysis are given in Sec. II. The numerical simulations are carried out in Sec. III. And Sec. IV is the conclusion.

[a)]Electronic mail: liuwhao@yeah.net.

II. THEORETICAL ANALYSIS

The schematic diagram is shown in Fig. 1: two sections of PWS, which is a parallel-plate waveguide with periodical corrugate profile in one of the plate, are placed along the path of the electron beam. The first PWS section (section-I) with larger size is for the pre-modulation of electron beam and the second PWS section (section-II) with smaller size is for the generation of terahertz wave radiation. These two sections are connected by a drift region, which is a smooth parallel-plate waveguide and is cutoff for the waves in section-I.

When the direct current electron beam (dc-beam) passes through section-I, the beam-wave interaction will be started and the beam velocity together with beam density will be modulated.[16–18] The modulation frequency, say ω_0, is determined by the structure parameters of section-I and the beam voltage. In the drift region, the beam density will be further modulated. According to the bunching theory,[19,20] besides the primary modulation component ω_0, there are lots of higher harmonic components in the modulated beam current.

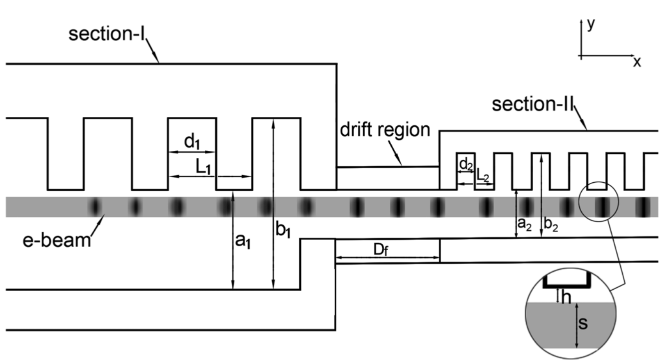

FIG. 1. Schematic diagram of the THz radiation source with two-section PWS. The shade variation in the figure indicates the process of charge density modulation of the electron beam.

These higher harmonic components result from the nonlinear beam-wave interaction in section-I as well as from the electron beam's further density modulation in the drift region. So, after passing through the drift region, the current density of the electron beam should be expressed as

$$J_x = \sum_{n=0}^{\infty} J_n e^{jn\omega_o t} = J_0 + J_1 e^{j\omega_0 t} + J_2 e^{j2\omega_0 t} + J_3 e^{j3\omega_0 t} + \ldots \quad (1)$$

in which the subscripts 0, 1, n (n = 2,3,…) indicate the dc component, basic modulation component, and *n-th* order harmonic component respectively. Usually, the amplitudes of the harmonics decrease gradually with the increase of the harmonic order ($J_0 > J_1 > J_2 > J_3 > \ldots$).

When the modulated electron beam is injected into section-II, the diffracted radiation (spontaneous radiation) will firstly be excited by the periodic boundary of PWS. And these diffracted waves then re-modulate the electron beam and start the beam-wave interaction (stimulated radiation) in section-II. If the operation frequency of section-II is just one of the harmonics of electron beam's pre-modulation frequency, the associated harmonic component in the beam current density will be exponentially amplified. The Pierce's theory about the traveling wave tube can be used to illustrate this process,[21] and the detailed mathematical manipulations will be omitted in the present paper for simplicity. Instead, we will use the theory of diffraction radiation from the PWS excited by a uniformly moving electron beam to show how the pre-modulated electron beam can reduce the starting current density of the beam-wave interaction in section-II.

The incident electric field (E_x^{in}) from the pre-modulated electron beam satisfies the nonhomogeneous Helmholtz equation:[22]

$$\nabla^2 E_x^{in} - \frac{1}{c^2}\frac{\partial^2 E_x^{in}}{\partial t^2} = -\mu\frac{\partial Jx}{\partial t} - \varepsilon\frac{\partial \rho}{\partial x}, \quad (2)$$

where c is the velocity of light in vacuum, ε and μ are, respectively, the permittivity and permeability of vacuum, ρ is the charge density and J_x is the beam current density expressed by Eq. (1). (They satisfy the continuous equation: $\frac{\partial\rho}{\partial t} = -\frac{\partial J_x}{\partial x}$.) Substituting Eq. (1) into Eq. (2), after the mathematical derivation we can get the incident electric field, which can also be expressed as the superposition of all harmonic components:

$$E_x^{in} = \sum_{n=0}^{\infty} E_n e^{jn\omega_0 t} = E_0 + E_1 e^{j\omega_0 t} + E_2 e^{j2\omega_0 t} + E_3 e^{j3\omega_0 t} + \ldots. \quad (3)$$

It shows that only the waves with frequencies of the harmonics of the pre-modulation frequency ($\omega = n\omega_0$) can generate diffraction radiation in section-II, which is just the condition for coherent radiation from the modulated electron beam.[15,23,24] The diffraction radiation frequency (ω_r) is determined by the coupling of the electron beam with the waveguide mode.[14] If the parameters of the structure and electron beam are chosen properly (to satisfy $\omega_r = n\omega_0$), the coherent radiation from the modulated electron beam can be obtained in section-II. And these coherent diffracted waves will re-modulate the electron beam and start the beam-wave interaction. Since the intensity of the coherent radiation from the modulated electron beam is significantly larger than that of the incoherent radiation from the dc-beam, the beam-wave interaction in section-II will be much easier to be started, and the starting current density will then be reduced. That is, by means of the two-section PWS, the high frequency terahertz radiation can be excited by an electron beam with moderate current density. The primary obstacle for the traditional vacuum electronic devices to generate high frequency terahertz radiation is then overcome.

The dispersion equations of the TM modes in the PWS, which interact with the longitudinally moving electron beam, can be expressed as (the coordinates and parameters are shown in Fig. 1 and we only consider the 2-D case, in which the field variation in 'z' direction is omitted)

$$\frac{-k}{k_{yn}}\sum_{n=-\infty}^{\infty}\frac{d_i}{L_i}\left[\frac{\sin(k_{xn}d_i/2)}{k_{xn}d_i/2}\right]^2 \cot k_{yn}a_i = \cot k(b_i - a_i), \quad (4)$$

where $k_{ym}^2 = k^2 - k_{xn}^2$, $k = \frac{\omega}{c}$, $k_{xn} = k_x + \frac{2n\pi}{L}$, subscripts $i = 1$ and $i = 2$, respectively, indicate the parameters of section-I and section-II as shown in Fig. 1. After optimization, the structure parameters of the two sections are set as $a_1 = 0.2$ *mm*, $d_1 = 0.05$ *mm*, $b_1 = 0.45$ *mm*, $L_1 = 0.1$ *mm*, and $a_2 = 0.06$ *mm*, $d_2 = 0.02$ *mm*, $b_2 = 0.14$ *mm*, $L_2 = 0.04$ *mm*. And the electron beam energy is set to be 10 kV. The calculated dispersion curves are shown in Fig. 2 (Fig. 2(a) and Fig. 2(b) signify the case of section-I and section-II, respectively). From Fig. 2(a) we can see that the frequency of beam-wave interaction in section-I is 0.27 THz, and it is also the basic modulation frequency of the electron beam ($\omega_0/2\pi$). Figure 2(b) shows the diffraction radiation frequency in section-II is 0.81 THz, which is exactly the third harmonic of the basic modulation frequency ($\omega_r = 3\omega_0$). So, according to the previous analysis, the coherent radiation will be obtained in section-II and the starting current density will be reduced. From the figure we can also see that the electron beams interact with the backward waves in both sections.

III. NUMERICAL SIMULATIONS

The numerical simulations are performed using CHIPIC, a finite-difference time-domain particle-in-cell electromagnetic solver.[25] And the simulation model is shown in Fig. 3(a). The dc-beam with current density 50 A/cm^2 and beam voltage 10 kV is injected from the left end of the structure. An external static magnetic field $B = B_0\hat{x}$ is used to transversely confine the beam. The PWS is set as perfect conductor and the open boundaries consist of perfectly matched layers. All the structure parameters are the same as that given in the theoretical analysis. The electron beam's phase-space distributions obtained by simulation are shown in Fig. 3(a) and Fig. 3(b). We can see that in both sections the velocity and charge density of the electron beam are efficiently modulated, which means that the beam-wave

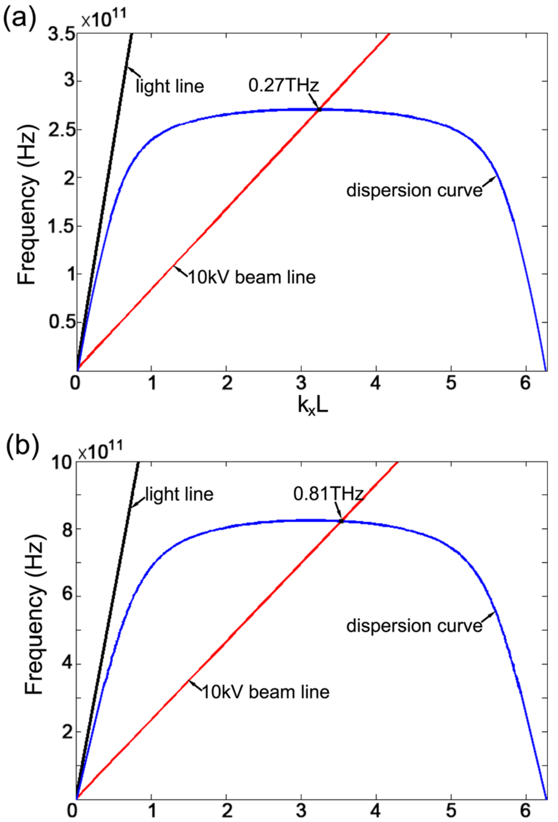

FIG. 2. (Dispersion curves of the waveguide modes (the lowest TM modes) in section-I (a) and section-II (b).

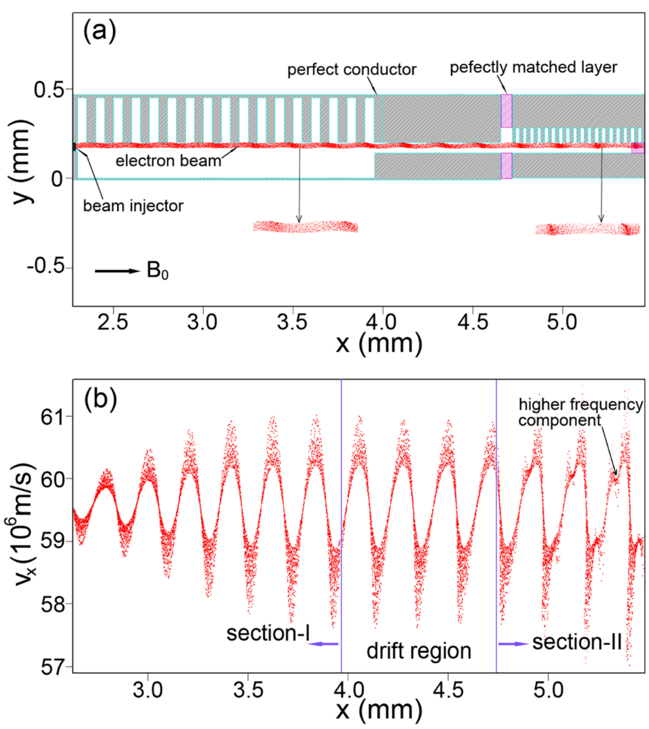

FIG. 3. (a) Simulation model used in CHIPIC together with the phase-space distribution of the electron beam in the structure, (b) The longitudinal velocity (v_x) of the electrons vs the longitudinal position x. (Snapshots of the phase-space distributions are taken at 7 ns.)

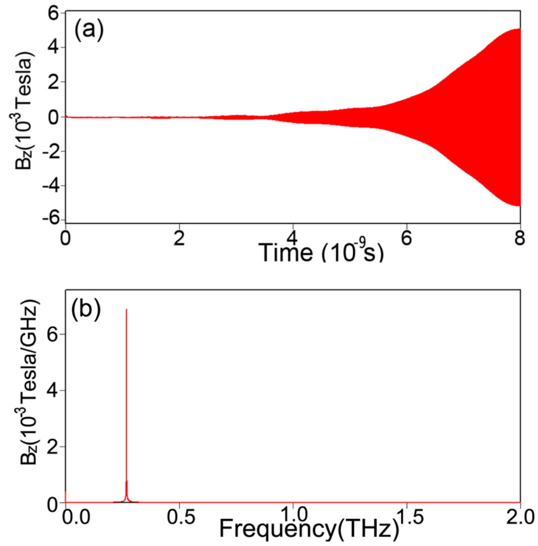

FIG. 4. Time evolution of the magnetic field B_z in section-I (a) and its frequency spectrum (b).

interactions are started in both sections. The velocity distribution of the electron beam in section-II indicates that the electron beam is further modulated by the higher frequency (compared with the pre-modulation frequency) waves excited in section-II (see Fig. 3(b)). The oscillating field (B_z) in section-I and its frequency spectrum are shown in Fig. 4, from which we can see that the frequency of the beam-wave interaction in section-I is 0.269 THz, agreeing well with the theoretical result. Figure 5 shows the current density and frequency spectrum of the electron beam, which has just passed through the drift region. Agreeing with the analysis, a series of higher harmonic components appear in the modulated electron beam and the magnitudes of them decrease gradually with the increase of the harmonic order.

The simulation results of the radiation wave in section-II and its frequency spectrum are given in Fig. 6, which shows that the radiation frequency is 0.808 THz, agreeing

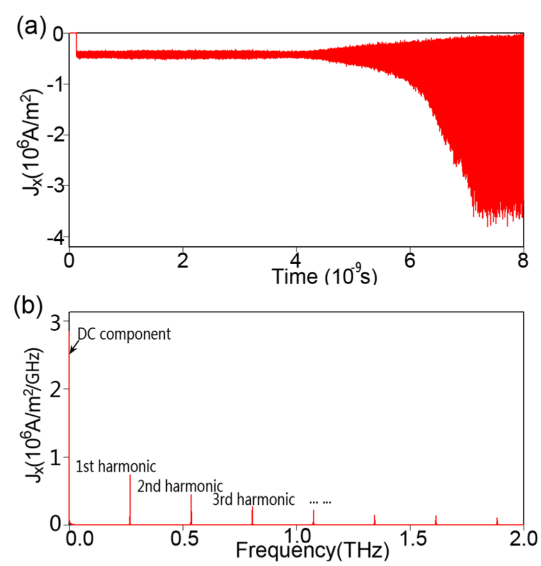

FIG. 5. Time evolution of the modulated beam current density J_x (a) and its frequency spectrum (b).

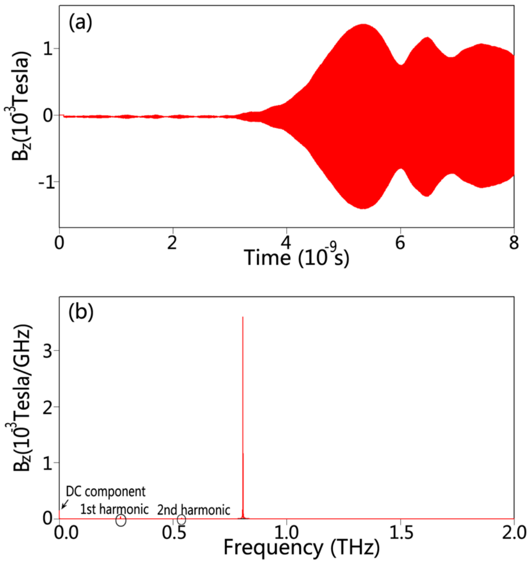

FIG. 6. Time evolution of the magnetic field B_z in section-II (a) and its frequency spectrum (b).

with the theoretical result. Besides the dominant radiation component, there are several other components (including the dc component, basic modulation component, and the 2nd harmonic component) in the detected wave, see Fig. 6(b). It can be understood that the probe used in simulation is not far enough away from the electron beam and the incident waves can also be detected. So, the waves shown in Fig. 6 are actually the superposition of the incident waves and the radiation waves in section-II.

Based on the analyses earlier, in order to get high power radiation in section-II, the electron beam should be efficiently pre-modulated before entering into section-II and the 3rd harmonic component of the beam current density should be as large as possible. The drift region plays an important role in the beam modulation. On one hand, it cannot be too short to effectively modulated the beam. On the other hand, it cannot be too long either, otherwise the bunched beam will collapse. The dependence of the 3rd harmonic component of the beam current density (after passing through the drift region) and of the radiation intensity in section-II on the drifting length (D_f) are shown in Fig. 7. From Fig. 7(a) we can see that, in the small scale ($0.5 < D_f/L_1 < 2$), there is one single peak, at $D_f = 0.75L_1$, for the radiation intensity, which means that 0.75 L_1 is the relative optimum value of the drift length. While Fig. 7(b) shows that, in the large scale ($1 < D_f/L_1 < 7$), both the 3rd harmonic component of the electron beam and the radiation intensity change periodically with the increase of drift length. It can be understood that the electron beam experiences the process of re-bunch and re-collapse periodically in the drift region.

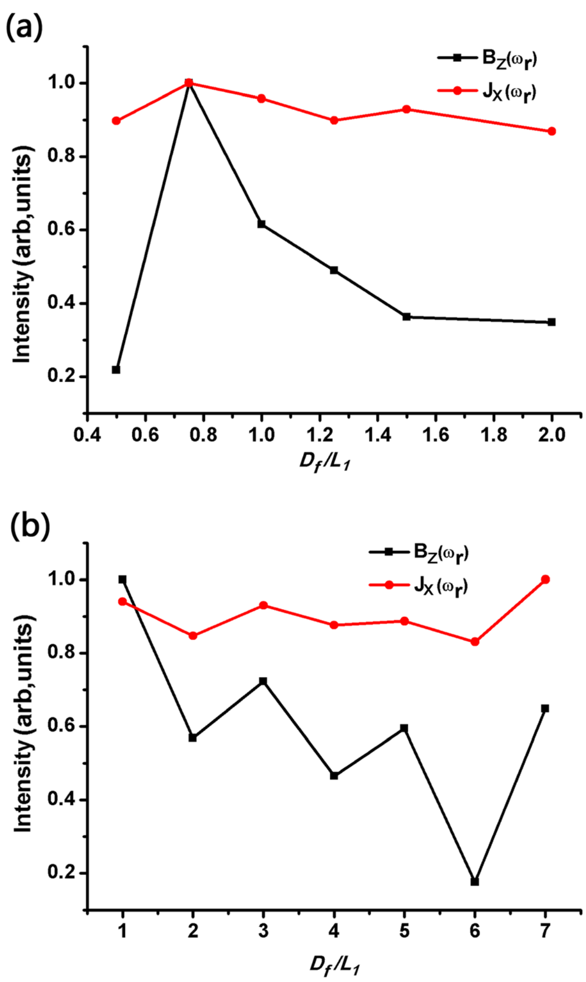

FIG. 7. The dependence of the 3rd harmonic component in the beam current density $J_x(\omega_r)$ and of the radiation field $B_z(\omega_r)$ on the drifting length. (a) is for the small scale and (b) is for the large scale.

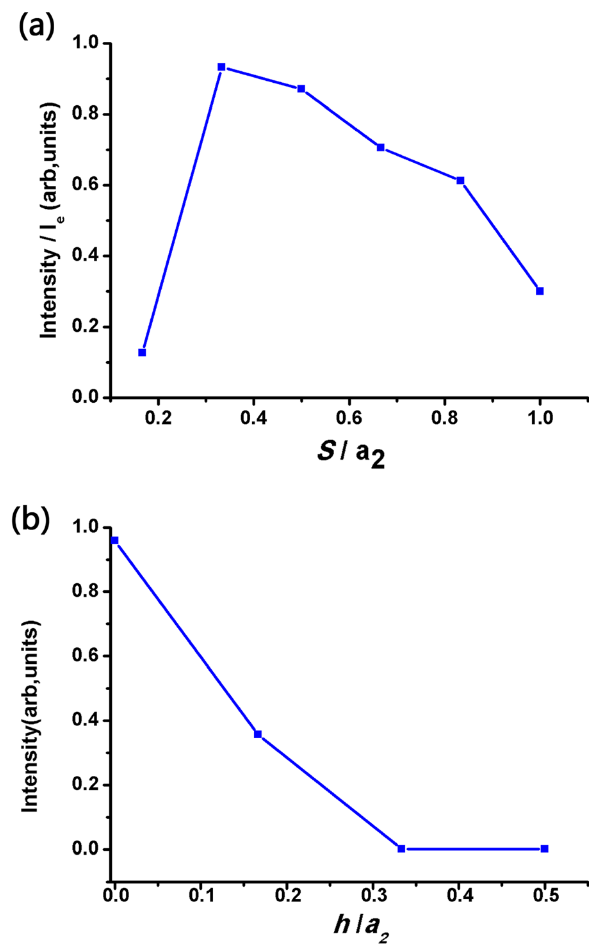

FIG. 8. The dependence of the radiation intensity on the beam thickness (a) and beam location (b). I_e in (a) means the total beam current.

The influences of the beam location (h shown in Fig. 1) and beam thickness (s) on the radiation intensity are given in Fig. 8. Figure 8(a) shows that there is an optimum value of beam thickness ($s = 0.3a_2$) to get the highest radiation efficiency. And Fig. 8(b) shows that the radiation intensity decreases exponentially with the increase of h, which is the typical feature of the diffraction radiation as well as the beam-wave interaction in the PWS.[13,14,20]

After optimizing the structure and electron beam parameters, the radiation with frequency higher than 0.8 THz and power over 0.5 W can be generated by a two-section PWS of one centimeter in width (in "z" direction). This power level is much higher than that from most of the available radiation sources in this frequency regime.

For comparison, we have carried out the simulation for the case that section-I is omitted and the results are shown in Fig. 9. (The beam current density is also 50 A/cm^2.) From the electrons' phase-space distribution shown in Figs. 9(a) and 9(b) we know that the electromagnetic oscillation is not started since the starting current density is not reached. And the intensity of the radiation wave in section-II, which is the incoherent diffraction radiation from the electron beam, is remarkably lower than that in the case section-I is present, see Figs. 9(c) and 9(d). Further simulations show that, without section-I, to start the beam-wave interaction in section-II, the beam current density should be higher than 200 A/cm^2, which is hard to achieve for the available technology.[26,27]

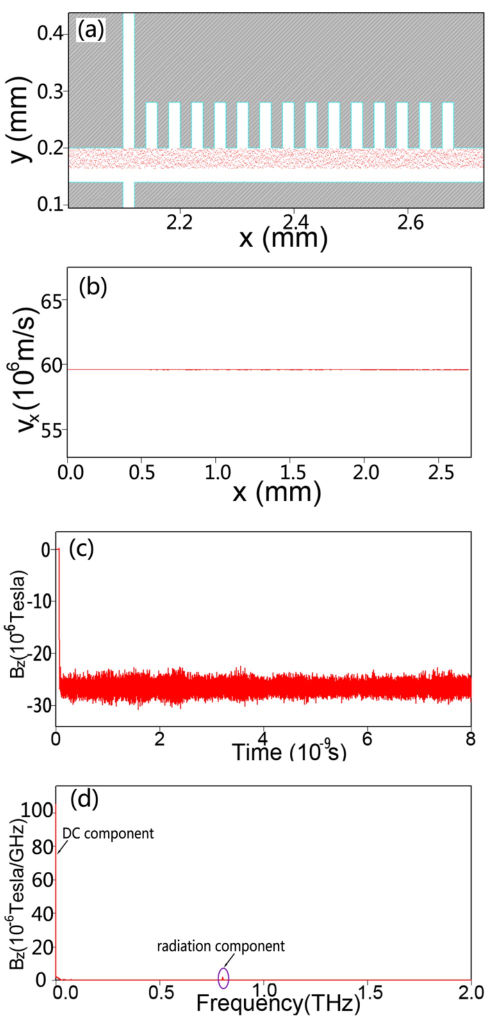

FIG. 9. Simulation results for the case that section-I is omitted. (a) and (b) are the electron's phase-space distributions in x-y space and $x - v_x$ space, respectively; (c) is the observed field B_z in section-II and (d) is its spectrum.

IV. CONCLUSION

To summarize, a kind of free electron terahertz wave radiation source using two-section PWS is proposed. Section-I is used to pre-modulate the electron beam and section-II is for terahertz wave generation. Both theoretical analysis and numerical simulations are carried out and their results are in agreement with each other. Our results show that the starting current density of the beam-wave interaction in section-II can be significantly reduced provided that its operation frequency is the harmonic of the pre-modulation frequency of the electron beam. And by use of the two-section PWS, the high frequency terahertz (frequency higher than 0.8 THz) wave radiation with power over 0.5 W can be excited by an electron beam with current density lower than 50 A/cm^2. This kind of source may have great potential application in developing the compact and high power terahertz wave radiation source.

ACKNOWLEDGMENTS

This work was supported by National Key Program of Fundamental Research of China under Contract No.2007CB310401, the National Natural Science Foundation of China under Contract No. 61001031, and the Fundamental Research Funds for the Central Universities under Contract No. ZYGX 2011J037.

[1]P. H. Siegel, IEEE Trans. M.T.T. **50**, 910–928 (2002).
[2]C. A. Schmuttenmaer, Int. J. Terahertz Sci. Technol. **1**, 1–8 (2008). Available at: http://www.tstnetwork.org/shownews1.asp?id=1.
[3]Y. M. Shin, J. Zhao, L. R. Barnett, and N. C. Luhmann, Phys. Plasmas **17**, 123105 (2010).
[4]J. H. Son, J. Appl. Phys. **105**, 102033 (2009).
[5]M. von Ortenberg, Int. J. Terahertz Sci. Technol. **1**, 9–21 (2008). Available at: http://www.tstnetwork.org/shownews1.asp?id=1.
[6]N. Laman, M. Bieler, and H. M. van Driel, J. Appl. Phys. **98**, 103507 (2005).
[7]Y. Ma, S. C. Saha, A. L. Bernassau, and D. R. S. Cumming, Int. J. Terahertz Sci. Technol. **4**, 85–86 (2011). Available at: http://www.tstnetwork.org/shownews1.asp?id=17.
[8]M. Lu, J. Shen, N. Li, Y. Zhang, C. Zhang, L. Liang, and X. Xu, J. Appl. Phys. **100**, 103104 (2006).
[9]E. Pickwell-MacPherson, Int. J. Terahertz Sci. Technol. **3**, 163 (2011). Available at: http://www.tstnetwork.org/shownews1.asp?id=12.
[10]Q. Qin, B. S. Williams, S. Kumar, J. L. Reno, and Q. Hu, Nature Photonics **3**, 732 (2009).
[11]M. Mineo and C. Paoloni, IEEE Trans. Electron Devices **57**, 1481 (2010).
[12]K. Zhang, Z. Wu, and S. Liu,. J. Infrared, Millimeter Terahertz Waves **30**, 309 (2009).
[13]G. Adamo, K. F. MacDonald, Y. Fu, C. M. Wang, D. P. Tsai, F. J. Garcia de Abajo, and N. I. Zheludev, Phys. Rev. Lett. **103**, 113901 (2009).
[14]S. Liu, M. Hu, Y. Zhang, W. Liu, P. Zhang, and J. Zhou, Phys. Rev. E. **83**, 066609 (2011).
[15]M. Hu, W. Liu, Y. Zhang, P. Zhang, J. Zhou, and S. Liu, Free-electron terahertz diffraction radiation source (unpublished).
[16]D. L. Webster, J. Appl. Phys. **10**, 864 (1939).
[17]J. A. Swegle, J. W. Poukey, and G. T. Leifeste, Phys. Fluids **28**, 2882 (1985).

[18]C. Prokop, P. Piot, M. C. Lin, and P. Stoltz, Appl. Phys. Lett. **96**, 151502 (2010).
[19]J. H. Fremlin, A. W. Gent, D. P. R. Petrie, P. J. Wallis, S. G. Tomlin, IEEE Journal **93**, 875–917 (1946).
[20]S. Liu *et al*., *Introduction of Microwave Electronics* (National Defense Industrial Press, Beijing, 1985), pp. 13–20 (in Chinese).
[21]J. R. Pierce, Proceedings of the IRE **35**, 111 (1947).
[22]K. Y. Ng, Phys. Rev. D **42**, 1819 (1990).
[23]Z. Shi, Z. Yang, F. Lan, X. Gao, Z. Liang, and D. Li, Nucl. Inst. Meth. Phys. Res. A **607**, 367 (2009).
[24]A. Gover, Phys. Rev. ST Accel. Beams **8**, 030701 (2005).
[25]J. Zhou, D. Liu, C. Liao, and Z. Li, IEEE Trans. Plasma Sci. **37**, 2002 (2009).
[26]K. T. Nguyen, J. A. Pasour, and T. M. Antonsen, IEEE Trans. Electron Devices **56**, 744 (2009).
[27]M. Mineo and C. Paoloni, IEEE International Vacuum Electronics Conference, 2011, (IVEC-2011), 265–266.